A New Principle of CNC Tool Path Planning for Three-Axis Sculptured Part Machining—A Steepest-Ascending Tool Path

Zezhong C. Chen
Department of Mechanical and Industrial Engineering,
Concordia University,
Montreal, Quebec, Canada, H3G 1M8

Geoffrey W. Vickers

Zuomin Dong

Department of Mechanical Engineering,
University of Victoria,
Victoria, BC, Canada V8W 3P6

Three-axis CNC milling is often used to machine sculptured parts. Due to the complex surface shape of these parts, well-planned tool paths can significantly increase the machining efficiency. In this work a new principle of CNC tool path planning for 3-axis sculptured surface machining is proposed. Generic formula to calculate the steepest tangent direction of a sculptured surface is derived, and the algorithm of the steepest-ascending tool path generation is introduced. A single steepest-ascending tool path has been verified to be more efficient than a single tool path of any other type. The relationship between machining efficiency and three key variables, tool feed direction, cutter shape, and surface shape, is revealed. The newly introduced principle is used in planning tool paths of a sculptured surface to demonstrate the advantages of the steepest-ascending tool paths. This new tool path scheme is further integrated into the more advanced steepest-directed and iso-cusped (SDIC) tool path generation technique. Applications of the new tool path principle and the SDIC tool paths to the machining of sculptured parts are demonstrated. [DOI: 10.1115/1.1765147]

1 Introduction

Mechanical parts with sculptured or free-formed surfaces, or sculptured parts, frequently finds applications in automotive, aeronautic, and naval industries, and even becomes popular in home electronics and appliances. These sculptured parts, such as dies and injection moulds, are usually machined on 3-axis CNC milling machines. Over the past decades a number of tool path planning approaches have been introduced for machining these sculptured surfaces [1]. These approaches have been created under two major assumptions: (a) the CNC machine and the cutter are both rigid enough so that the cutter deflection and deformation can be ignored; and (b) the surface shape of a sculptured part is formed by point-to-point cutting. The major objective of automated planning and programming for CNC machining is to obtain the balance on the quality of the machined surface and the machining time. Some of the previous studies considered computational efficiency, consistency of surface roughness, redundant machining, and surface tolerance. These representative schemes for tool path generation follow the principles of *iso-parametric, non-constant parameter, iso-phote, iso-cusped,* and *steepest directed tree*. The iso-parametric tool path generation method creates an iso-parametric tool path by fixing one surface parameter and varying the other surface parameter. The cross-feed distance between two adjacent iso-parametric tool paths remains constant throughout the paths [2,3]. The non-constant parameter CNC tool path generation method intersects a family of parallel planes with the part surface, and each intersection curve becomes a tool path [4]. The major advantage of these two methods is the ease of computation in automated tool path planning and programming. The iso-phote CNC tool path generation method creates a new tool path segment by continuously checking and eliminating possible interferences with previously created tool path segments [5]. The iso-cusped tool path generation method evenly distributes tool paths across the surface to make sure that the cusps are of equal height and thereby eliminates redundant machining [6–8]. The steepest directed tree tool path generation method defines tool paths by connecting the nodes of generated surface mesh to climb the geometry features in a steepest way [9]. One common drawback of these tool path generation methods is that the created cutter paths cannot ensure to remove the maximum amount of stock material in each tool motion step if the tool feed rate and the step length are fixed. Two reasons contributed to the problem: (a) the amount of material removed in each step depends on the tool feed direction; and (b) the tool feed direction in these tool paths constantly changes.

To solve this problem, a new principle to plan an efficient tool path is proposed. The generic formula to calculate the steepest tangent direction of any sculptured surface is derived. The algorithm of a steepest-ascending tool path generation is introduced. To verify that a single steepest-ascending tool path is the most efficient tool path, the lengths of the effective cutting edges of three commonly-used milling cutters, ball, torus, and flat end-mills, are calculated in different tool feed directions [10,11]. This new tool path generation principle is applied to a sculptured part defined by a NURBS surface in its CNC tool path generation. The example part is machined using the created steepest-ascending tool paths on a DECKEL MAHO 60T CNC machine to verify its advantages. The steepest-ascending tool paths are further adopted in the integrated steepest-directed and iso-cusped (SDIC) tool path generation algorithm [12]. The example of SDIC tool paths clearly demonstrates the superior machining efficiency of the steepest-ascending tool paths.

2 Steepest Tangent Direction of a Sculptured Surface at a Cutter Contact Point

For a sculptured surface in 3-D space, there exists only one steepest tangent direction at any given surface point. The generic formula of the steepest tangent direction of a sculptured surface is derived in this section. Suppose a surface, S, defined in parametric form and a *cutter contact* (CC) point, P_0, on the surface, as shown in Fig. 1, can be expressed as [13]

Contributed by the Manufacturing Engineering Division for publication in the JOURNAL OF MANUFACTURING SCIENCE AND ENGINEERING. Manuscript received Jan. 2004. Associate Editor: M. Davies.

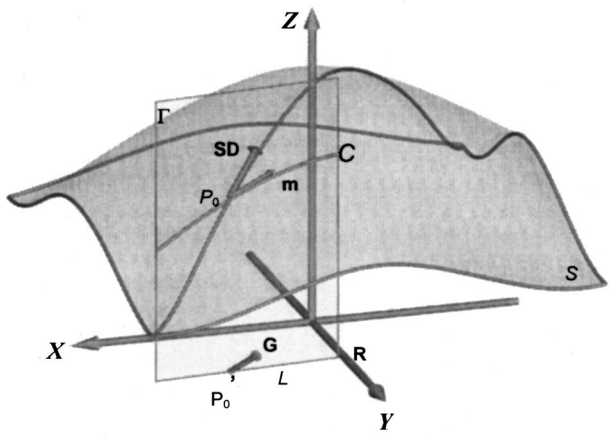

Fig. 1 Steepest tangent direction of a surface at a cutter contact point

$$S:\mathbf{S}(u,v)=\begin{bmatrix} x(u,v) \\ y(u,v) \\ z(u,v) \end{bmatrix} \tag{1}$$

$$P_0:\mathbf{P}(u_0,v_0)=\begin{bmatrix} x(u_0,v_0) \\ y(u_0,v_0) \\ z(u_0,v_0) \end{bmatrix} \tag{2}$$

This parametric representation of the surface can be transformed into analytic form as $z=z(x,y)$ with assistance of Eq. (3) and Eq. (4) [14].

$$\frac{\partial z}{\partial x}=-\frac{\mathbf{D}[y,z]}{\partial(u,v)}\Big/\frac{\mathbf{D}[x,y]}{\partial(u,v)} \tag{3}$$

$$\frac{\partial z}{\partial y}=\frac{\mathbf{D}[x,z]}{\partial(u,v)}\Big/\frac{\mathbf{D}[x,y]}{\partial(u,v)} \tag{4}$$

While, $\mathbf{D}[x,y]/\partial(u,v)$, $\mathbf{D}[y,z]/\partial(u,v)$ and $\mathbf{D}[x,z]/\partial(u,v)$ are Jacobian determinants, having the form

$$\frac{\mathbf{D}[y,z]}{\partial(u,v)}=\begin{vmatrix} \frac{\partial y}{\partial u} & \frac{\partial z}{\partial u} \\ \frac{\partial y}{\partial v} & \frac{\partial z}{\partial v} \end{vmatrix} \tag{5}$$

$$\frac{\mathbf{D}[x,z]}{\partial(u,v)}=\begin{vmatrix} \frac{\partial x}{\partial u} & \frac{\partial z}{\partial u} \\ \frac{\partial x}{\partial v} & \frac{\partial z}{\partial v} \end{vmatrix} \tag{6}$$

$$\frac{\mathbf{D}[x,y]}{\partial(u,v)}=\begin{vmatrix} \frac{\partial x}{\partial u} & \frac{\partial y}{\partial u} \\ \frac{\partial x}{\partial v} & \frac{\partial y}{\partial v} \end{vmatrix} \tag{7}$$

From Eqs. (3) and (4), the steepest tangent direction of a surface can be derived. Projecting the CC point, P_0, vertically onto the XOY plane leads to its projection, P_0', and $\mathbf{P}_0'=[x_0,y_0,z_0]^T=[x(u_0,v_0),y(u_0,v_0),0]^T$, as illustrated in Fig. 1. Assume a line, L, is crossing point P_0' on the XOY plane, and the direction of this line is represented as $\mathbf{R}=[a,b,0]^T$. Line L can thus be represented as

$$L:\begin{bmatrix} x \\ y \\ z \end{bmatrix}=\mathbf{P}_0'+t\cdot\mathbf{R}=\begin{bmatrix} x_0 \\ y_0 \\ 0 \end{bmatrix}+t\cdot\begin{bmatrix} a \\ b \\ 0 \end{bmatrix}=\begin{bmatrix} x_0+at \\ y_0+bt \\ 0 \end{bmatrix} \tag{8}$$

Now, a vertical plane, $\mathbf{\Gamma}$, passes through line L can be introduced as shown in Fig. 1. The intersection curve, C, between plane $\mathbf{\Gamma}$ and the surface S can be obtained from the following:

$$\begin{cases} x=x_0+at \\ y=y_0+bt \\ z=z(x,y) \end{cases} \tag{9}$$

Since this intersection curve can be represented as a parametric curve of t, the tangent of the intersection curve C, at the CC point, P_0, can be obtained from

$$\left.\frac{\partial x}{\partial t}\right|_{P_0}=a,\left.\frac{\partial y}{\partial t}\right|_{P_0}=b,\quad \text{and}\quad \left.\frac{\partial z}{\partial t}\right|_{P_0}=\left.\left(a\cdot\frac{\partial z}{\partial x}+b\cdot\frac{\partial z}{\partial y}\right)\right|_{P_0} \tag{10}$$

A vector, $\mathbf{m}$, along the tangent direction of the surface then takes the form

$$\mathbf{m}=\left[a,b,a\cdot\frac{\partial z}{\partial x}+b\cdot\frac{\partial z}{\partial y}\right]^T \tag{11}$$

The direction of this tangent vector, $\mathbf{m}$, is used as the tool feed direction. Its directional derivative and gradient formula can be deducted based on computational geometry [15]. For the surface S given in its analytic form, $z=z(x,y)$, its gradient, $\mathbf{G}$, at the CC point is $[\partial z/\partial x,\partial z/\partial y,0]^T$, and the direction derivative of the surface function, $z=z(x,y)$, along the direction of $\mathbf{R}$ is obtained as

$$|\nabla z|=\mathbf{G}^T\cdot\mathbf{R}=\begin{bmatrix} \frac{\partial z}{\partial x} & \frac{\partial z}{\partial y} & 0 \end{bmatrix}\cdot\begin{bmatrix} a \\ b \\ 0 \end{bmatrix}=a\cdot\frac{\partial z}{\partial x}+b\cdot\frac{\partial z}{\partial y} \tag{12}$$

Comparing Eqs. (10) and (12), the directional derivative of the surface along the direction, $\mathbf{R}$, equals the Z component of the tool feed direction, $\mathbf{m}$. The directional derivative physically means the projection of the surface gradient, $\mathbf{G}$, at the CC point, P_0, to the direction $\mathbf{R}$. The Z component of the tool feed direction, $\mathbf{m}$, reflects the slope of the direction.

From geometric projection point of view, the directional derivative reaches the maximum when the free direction, $\mathbf{R}$, is in line with the gradient, $\mathbf{G}$; in other words, when $\mathbf{R}=\mathbf{G}=[\partial z/\partial x,\partial z/\partial y,0]^T$, the directional derivative is $|\nabla z|=(\partial z/\partial x)^2+(\partial z/\partial y)^2$. In this case, the Z component of the tool feed direction reaches the maximum; therefore, the tool feed direction is the steepest. The steepest tangent direction can thus be obtained. When rotating the plane, $\mathbf{\Gamma}$, along the axis P_0P_0', from a direction, $\mathbf{R}$, to the surface gradient, $\mathbf{G}$, the intersection curve, C, between the plane, $\mathbf{\Gamma}$, and the surface, S, is changed accordingly. At last when the direction, $\mathbf{R}$, is aligned with the surface gradient, $\mathbf{G}$, the tool feed direction, $\mathbf{m}$, becomes the steepest tangent direction, $\mathbf{SD}$, at the CC point, P_0, (see Fig. 1). Thus the steepest tangent direction, $\mathbf{SD}$, at the CC point, P_0, on a surface, $z=z(x,y)$, has the following generic form

$$\mathbf{SD}=\left[\frac{\partial z}{\partial x},\frac{\partial z}{\partial y},\left(\frac{\partial z}{\partial x}\right)^2+\left(\frac{\partial z}{\partial y}\right)^2\right]^T \tag{13}$$

3 A Steepest-Ascending Tool Path

A steepest-ascending tool path generates a trail of CC points from the bottom to the top of the surface, and the tangent vector of the path is along the steepest tangent direction at each CC point. Two tool paths of this type are illustrated in Fig. 2, and the tool moves from a lower corner to the top of the surface along a steepest-ascending tool path, not moving down from the top to the bottom. The steepest tangent direction expression, $\mathbf{SD}$, given in Eq. (13), indicates that once the part is fixed on a 3-axis CNC

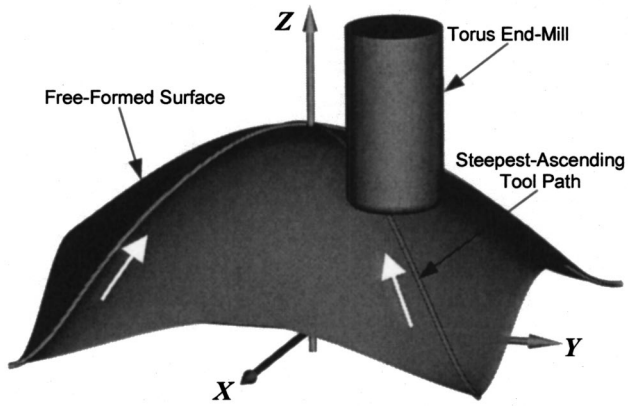

Fig. 2 Steepest-ascending tool paths for a sculptured surface

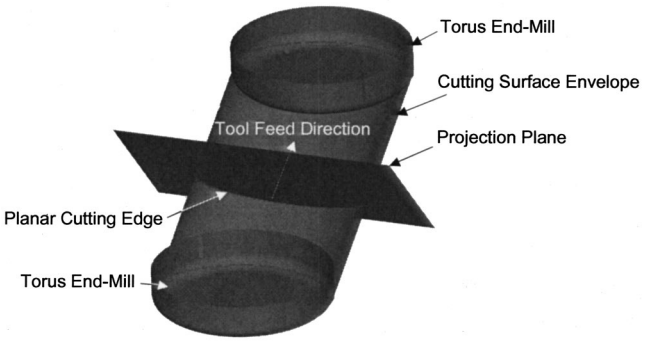

Fig. 3 A generic machining model of torus end-mill

machine, there exists only one steepest tangent direction at any CC point. Therefore, the steepest-ascending tool path can be uniquely determined if a starting point at the bottom of the surface is given.

Each steepest-ascending tool path is represented by a set of CC points placed sequentially on surface contours. The procedure for finding a steepest-ascending tool path of a surface is given below.

1) Generate a contour map surface model of the sculptured part. The surface contours are to be created on planes that are perpendicular to the cutter axis, and the number of contours is adjustable according to the specified surface tolerance.

2) Choose a CC point on the lower bound of the sculptured surface as the starting point of the tool path, and calculate the surface gradient at that point. On the contour map model, generate a vector using the CC point and its gradient direction.

3) Find the intersection between the vector and the next higher contour curve. This intersection is used as the next CC point. Unless the present surface contour is at the top of the surface model, take the newly obtained CC point as a new starting CC point and then go to Step (2). Otherwise, go to the step 4).

4) Connect all CC points identified in steps 1) to 3) to form a steepest-ascending tool path.

4 A New Tool Path Generation Principle and Its Verification

4.1 A New Principle in 3-Axis CNC Machining. According to the definition of the steepest-ascending tool path, the tool feed direction in each cutter motion is along the steepest tangent and upwards direction if the cutter moves along this tool path. It has been proven that for 3-axis CNC machining a cutter has highest machining efficiency in each tool path step if the cutter moves along the steepest tangent direction [10,11]. Thus, a single steepest ascending tool path is the most efficient tool path, which means the cutter machines a strip on the surface along the path and its neighboring sides at maximum rate. This is the new principle for 3-axis CNC tool path planning. The principle is not applicable to 4- or 5-axis machining because the cutter may not have maximum efficiency by simply move it along the steepest tangent direction. In addition, although the stated principle services as a guideline to the planning of an efficient tool path, it could not eliminate gouging and interference in the CNC machining of a complex sculptured surface.

To verify this principle, a measure of machining efficiency, effective cutting edge, is introduced. Calculation on the length of the effective cutting edge is demonstrated using an example of machining a hemi-cylindrical part. The relationships between machining efficiency and the three key influencing factors, tool feed direction, tool shape and surface shape, are provided.

4.2 Effective Cutting Edge. To define a measure on machining efficiency, a generic machining model is introduced to define the effective cutting edge. In this machining model, a 3-axis vertical CNC machine is used to machine a sculptured surface. The machine and tool are assumed to be rigid enough to ignore cutter deflection and deformation during cutting. Along each tool path the three-axis CNC machining is carried out through many tool motions. A torus end-mill, or bull-nose mill, is used in this model as the generic cutter. When the cutter moves from one CC point to another, an envelope of the torus-shaped cutting surface is generated as shown in Fig. 3. If a planar cutting edge is defined as the profile of the cutter projected onto a plane normal to the cutter feed direction, the envelope of the cutting surface can be formed by sliding the planar cutting edge along the cutter feed direction, as illustrated in Fig. 3. The *effective cutting edge* (ECE) is defined as the portion of the planar cutting edge between the sculptured surface and tolerance surface, which is an offset of the sculptured surface by the surface tolerance as shown in Fig. 4 [10]. In this figure the sculptured surface is represented as a curve that is the intersection of the projection plane and the sculptured surface; similarly the curve of the tolerance surface is the intersection between the projection plane and the tolerance surface. The shape and length of the effective cutting edge is then illustrated by the curve segment between the curves representing the part surface and tolerance surface, as shown in Fig. 4. The ECE determines the local surface quality and the cutting rate in the tool motion.

In one cutter motion, all stock material above and inside the envelope is removed. If the cutter feed rate and the step length (or motion distance) are fixed, increasing the length of ECE allows more stock material to be removed in one tool motion step. The cutting is more efficient. So the length of ECE is a measure of machining efficiency.

4.3 ECE Length vs. Tool Feed Direction. Machining efficiency is a function of the tool feed direction. The closer the tool feed direction is to the steepest tangent direction on the sculptured surface, the longer the ECE length, and therefore the higher the

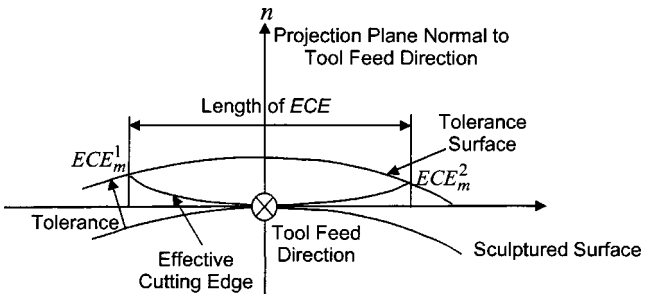

Fig. 4 Effective cutting edge and its length

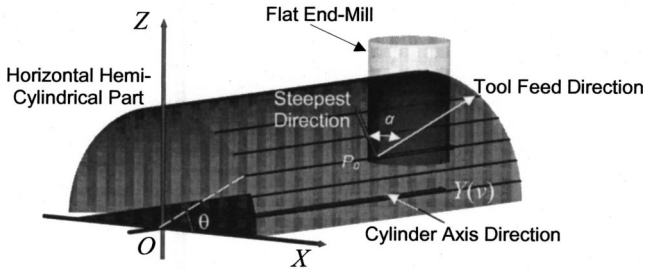

Fig. 5 Horizontal cylinder and tool feed directions

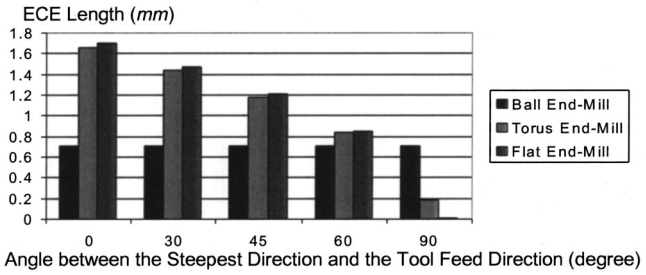

Fig. 6 ECE lengths of three cutters in five tool feed directions

machining efficiency. To illustrate this relationship, the calculated ECE lengths of an example part at different tool feed directions is given. The part has a horizontal cylindrical shape, represented in a parametric form, $S(0,v)$, with a radius of 50 mm and a length of 100 mm. This part is machined using the three commonly used cutters, a ball end-mill (or ball-nose mill), a flat end-mill, and a torus end-mill, respectively. The radius of these cutters is 6.35 mm; the fillet radius of the torus end-mill is 0.45 mm; and the surface tolerance is 0.01 mm. The cutter is positioned at a CC point $P_0(80°,50)$, where angle θ is at 80° and the Y coordinate along the cylinder length is 50 mm. The angle α (shown in Fig. 5) is the angle between the tool feed direction and the steepest tangent direction at the CC point. The ECE length is studied for several different given α values, including 0°, 30°, 45°, 60° and 90°.

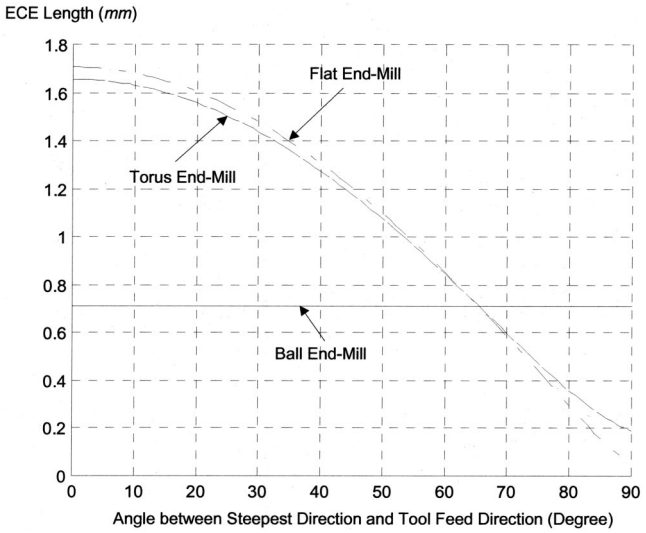

Fig. 7 Relationship between ECE length and tool feed direction at CC point (80°,50)

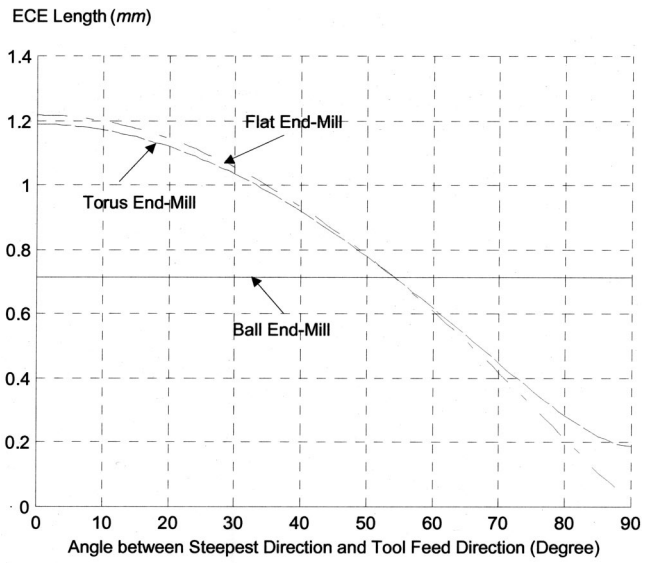

Fig. 8 Relationship between ECE length and tool feed direction at CC point (70°,50)

The ECE lengths for these cutters moving along the tool feed directions defined as above are calculated and given in Fig. 6. For the ball end-mill the ECE length is independent from the tool feed direction, because the envelope of a sphere shape cutting surface remains as a part of a cylindrical surface, independent to the tool feed direction; and the shape of the ECE is always a circular arc with the radius of the cutter. The ECE length of the flat end-mill is the most sensitive to the tool feed direction. The torus end-mill always falls between the two although its dimensions given in this example are quite close to the flat end-mill.

As shown in Fig. 6 the longest ECE length of 1.7065 mm occurs when the flat end-mill moves along the steepest pathway (i.e. $\alpha=0°$). The ECE length of the flat end-mill drops dramatically when the tool feed direction diverts from the steepest pathway. For instance, when the angle α is 90°, indicating the tool feed direction is perpendicular to the steepest tangent direction,

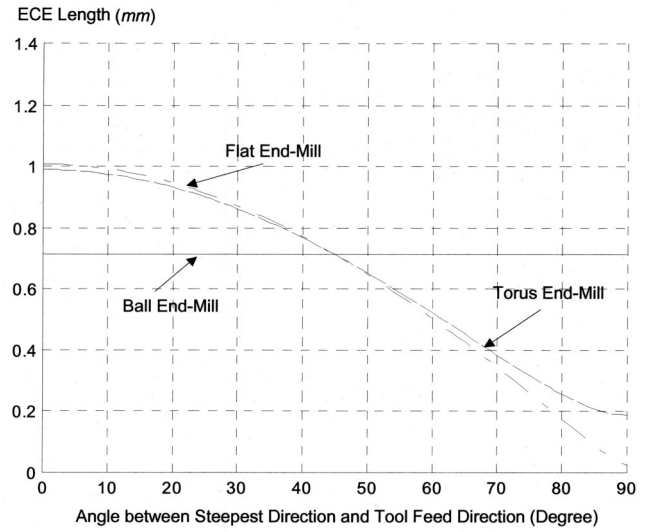

Fig. 9 Relationship between ECE length and tool feed direction at CC point (60°,50)

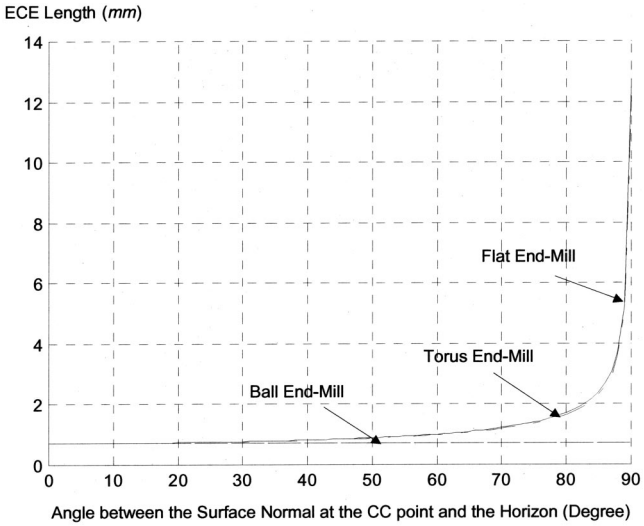

Fig. 10 Relationship between the ECE length and CC points

the ECE length of the flat end-mill drops to 0.0058 mm—a factor of 285 to 1. Likewise, the ECE length of the torus end-mill at this angle drops by a factor about 9 to 1.

With the steepest pathway movement (i.e. $\alpha=0°$), the ECE lengths of the flat end-mill and the torus end-mill are 2.4 and 2.3 times larger respectively than that of the ball end-mill.

4.4 Machining Efficiency and Three Major Influencing Factors. To further illustrate the relationship between machining efficiency and the three key influencing factors (tool feed direction, tool shape, and surface shape), a set of curves for ball, torus, and flat end-mills located at three positions (angle θ is 80°, 70°, and 60°) on the hemi-cylindrical part are given in Figs. 7, 8, and 9, respectively. The ECE lengths of the three different mills at each surface position for all tool feed directions are presented. The solid line represents the ECE length of the ball end-mill; the dashed line represents the ECE length of the torus end-mill; and the dash-dotted line represents the ECE length of the flat end-mill.

As shown in these figures ECE length is not only related to the tool feed direction and tool shape, but also the direction of the surface normal. At point (80°,50) the ECE length of the flat end-mill moving in the steepest direction is 1.7065 mm and 2.4 times longer than the ball end-mill as shown in Fig. 7. At point (70°,50) the ECE length is reduced to 1.217 mm and 1.7 times longer than the ball end-mill as shown in Fig. 8. At point (60°,50) the ECE length is reduced to 1.007 mm and only 1.4 times longer than the ball end-mill as shown in Fig. 9. In other words, as the orientation of the surface normal approaches the cutter axis direction, the ECE length reaches its maximum. In all three cases the torus end-mill falls between the ball and flat end-mills.

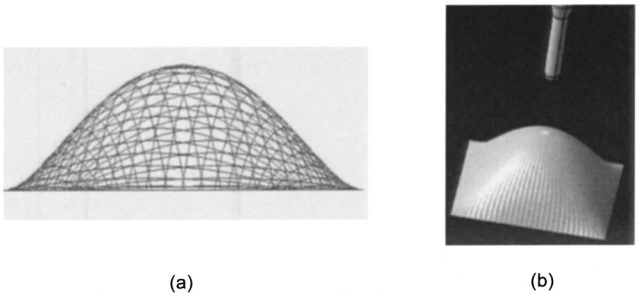

Fig. 11 (a) Sculptured part; (b) steepest-ascending tool paths of the sculptured part

For the steepest pathways and those reasonably close to the steepest pathways, the flat and torus end-mills are always superior to ball end-mills. However, if the tool feed direction is allowed to divert significantly from steepest tangent direction the ECE length of the flat and torus end-mill is reduced below that of the ball end-mill. The breakeven point is reduced as the steepness of the surface is increased.

The effect of cutter position on the part is summarized in Fig. 10. When the CC point moves from point (0°,50) at the bottom to point (90°,50) at the top of the cylinder, the ECE length of the flat end-mill increases exponentially. The ratio of ECE length between the flat end-mill and ball end-mill increases from 1 at point (0°,50) to 18 at point (90°,50). In particular, when α value varies between 80° to 90° (i.e. a relatively smooth surface of the sort encountered in a propeller or an automotive body panel), the ECE length ratio between the flat end-mill and the ball end-mill will be between 2.4 and 18 times for 3-axis CNC machining. Appropriate selection of cutting tool becomes crucially important.

5 Applications of Steepest-Ascending Tool Paths

5.1 An Example Sculptured Part. To demonstrate the efficiency benefit of the steepest-ascending tool path, the new tool path planning principle has been applied on a sculptured part that is designed using a NURBS surface on CATIA v5 CAD/CAM system, and the part is shown in Fig. 11(a). The newly introduced steepest-ascending tool path generation algorithm has been implemented in an automated tool path generation program and used to

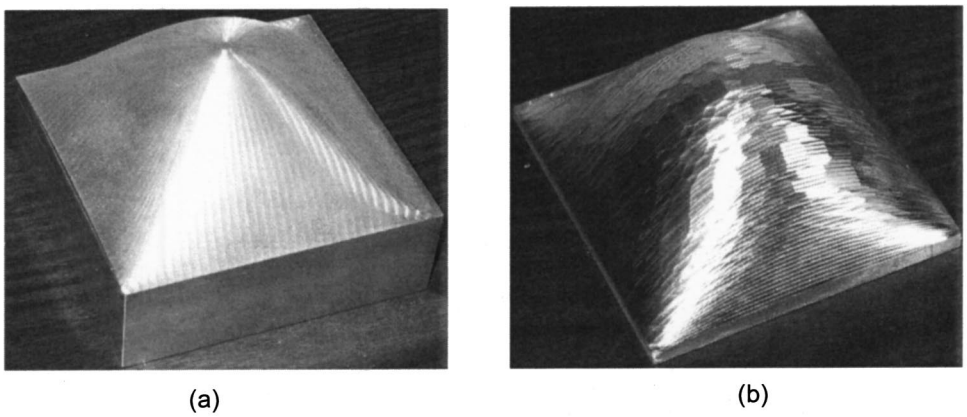

Fig. 12 (a) Machined part with steepest-ascending tool paths; (b) machined part with tool paths generated with CATIA system

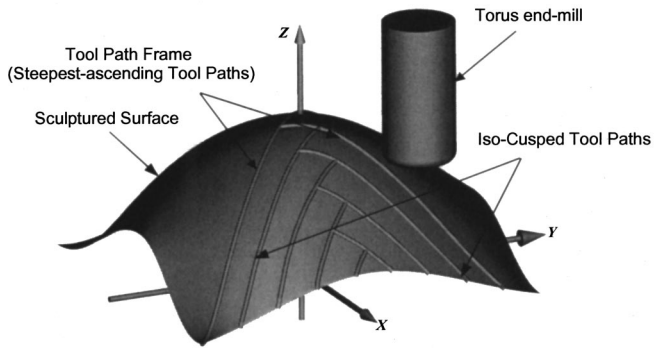

Fig. 13 SDIC tool paths of a sculptured surface

generate the steepest-ascending CNC tool paths for the presented example. Machining of this part using the generated tool paths is first simulated using the CNC simulation function of CATIA, as shown in Fig. 11(b). A DECKEL MAHO 60T CNC milling machine is then used to machine the part with the steepest-ascending tool paths. The material of the part is aluminum. A high-speed-steel flat end-mill with diameter of 12.7 mm is used in its rough and finish machining with a cutting feedrate of 1000 mm/min, and a spindle speed of 1000 r/min. The machined part is shown in Fig. 12(a).

To demonstrate the advantage of the steepest-ascending tool paths, CNC tool paths for machining this part are also generated using the manufacturing module of CATIA. The part is machined under identical conditions using CATIA's tool paths. The finished part is shown in Fig. 12(b). The two sets of tool paths lead to different results:

• The total length of the steepest-ascending tool paths is about 20% shorter than the total length of the tool paths generated using CATIA. Thus the machining time of the steepest-ascending tool paths is about 20% less, leading to the improved machining productivity.

• The surface quality of the part machined using the steepest-ascending tool paths is noticeably superior as shown in Fig. 12.

The primary reason for the superior performance of the steepest-ascending tool paths is due to the fact that its tool paths are prevented to divert away from the steepest tangent direction at the cutter contact points through out the surface, while the others are not.

5.2 Integrated Steepest-Directed and Iso-Cusped Tool Path Method. The steepest-ascending tool path has been integrated into an advanced optimum tool path generation approach—the steepest-directed and iso-cusped (SDIC) tool paths. The principle of SDIC and its uniqueness are briefly outlined. CNC machining on the previously defined hemi-cylindrical example part is used to illustrate this advanced tool path generation method and its advantages.

A steepest-ascending tool path is productive because the machining capacity of the tool reaches maximum when the tool cuts along the steepest tangent direction. However, a series of adjacent steepest-ascending tool paths can cause redundant machining where the tool paths are unnecessarily dense for a given surface tolerance. On the other hand, the iso-cusped tool paths are efficient due to the non-existence of redundant machining. However to maintain the equal cusp, the tool path pathways will slowly deviate from the steepest direction, and the overall machining efficiency of the tool paths is reduced. The search for a better solution that combines the two tool path generation principles inherits their advantages and avoids their drawbacks lead to the introduction of the SDIC tool path generation method. In short, the SDIC approach uses a number of steepest-ascending tool paths to form the guiding frame or skeleton across the sculptured surface, and fills the surface area inside of each frame using offsetting iso-cusp tool paths.

In Fig. 13, two steepest-ascending tool paths starting from the two bottom corners of the surface establish the boundaries of the guiding frame, and the iso-cusped tool paths are generated to cover the enclosed region by offsetting sequentially from each side of the boundary, forming an interlaced pattern. The steepest-ascending tool paths control the direction trends of the iso-cusped

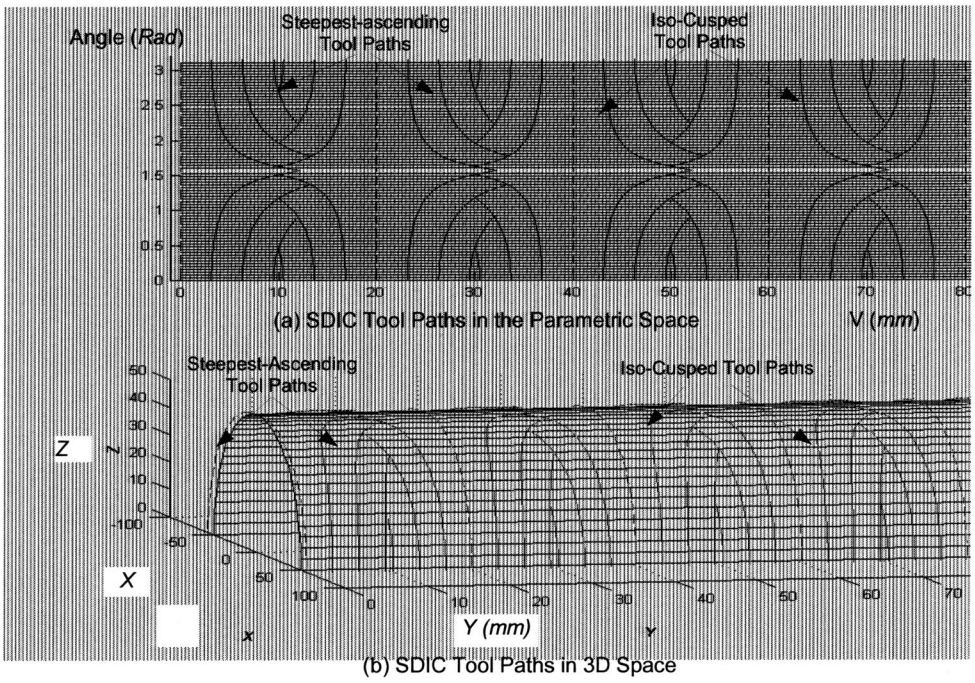

Fig. 14 SDIC tool paths of the hemi-cylindrical part

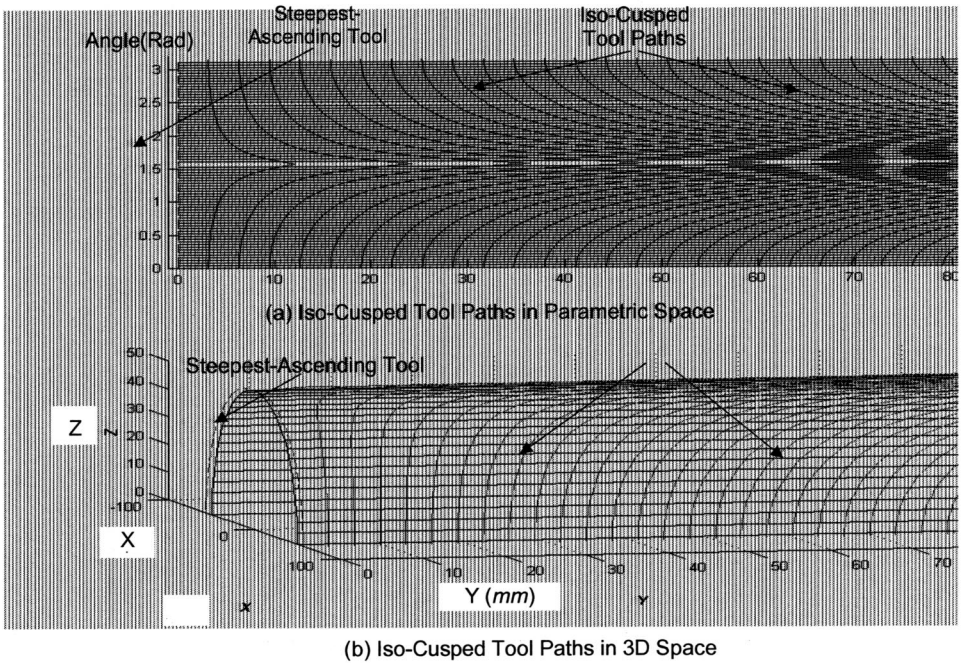

Fig. 15 SDIC tool paths with a frame of one steepest-ascending tool path

tool paths so that the possibility of their straying too far from the steepest tangent direction is reduced. The iso-cusped tool paths are evenly distributed in the region between two neighboring steepest-ascending tool paths and the extent of repetitive machining is significantly decreased. The number of steepest-directed tool paths that define the guiding frame can be optimized according to minimum tool path length; although a close-form solution would be very difficult due to the complexity of the surface.

5.3 A Case Study. To illustrate the SDIC approach the hemi-cylindrical part, shown in Fig. 5, is used again. The surface machining tolerance has been increased to 0.1 mm for the ease of illustration; a flat end-milling cutter of 6.35 mm radius is used; and six steepest-ascending frame tool paths are used. The SDIC approach was implemented using MATLAB on a DELL Dimension XPS 500. The generated SDIC tool paths for this part are shown in Fig. 14.

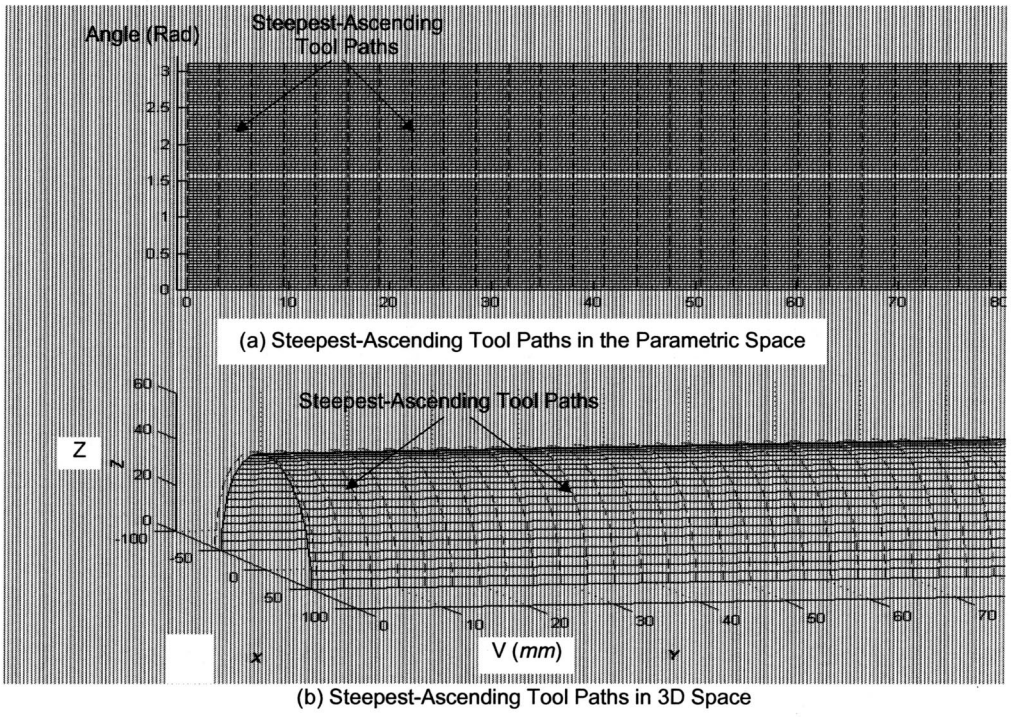

Fig. 16 SDIC tool paths with a frame of 33 steepest-ascending tool paths

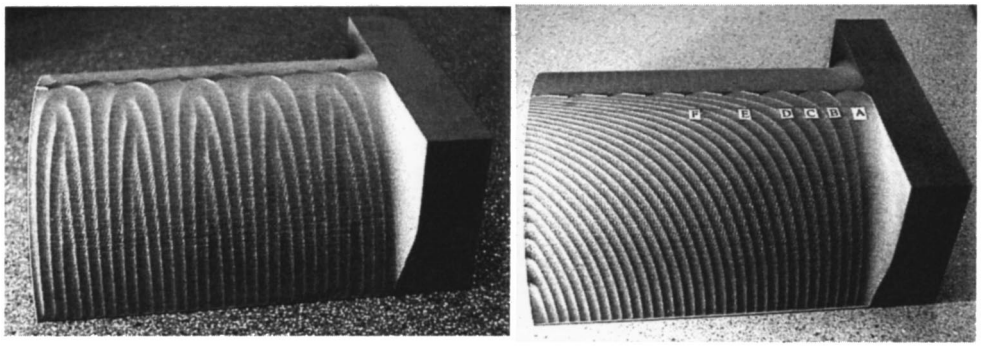

(a) SDIC Tool Paths

(b) Iso-Cusped Tool Paths

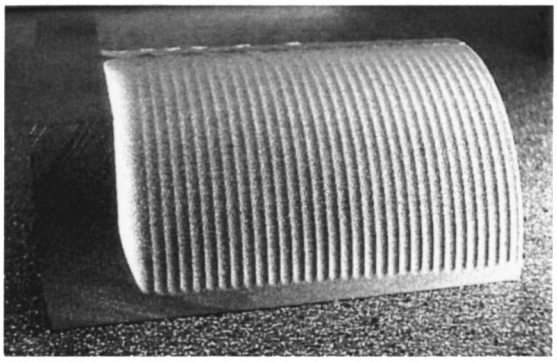

(c) Steepest-Ascending Tool Paths

Fig. 17 Three types of tool paths for the hemi-cylindrical part

In Fig. 14(a) the SDIC tool paths are presented in parametric space with two parameters (sectional circular angle θ, cylinder length v). The six dashed lines are the steepest-ascending tool paths evenly distributed along the cylinder, and the thirty curved solid lines are the isocusped tool paths. These SDIC tool paths are further shown in the 3-D Cartesian space in Fig. 14(b). The total length of these SDIC tool paths is 4472 mm.

With different numbers of the steepest-ascending frame tool paths, a variety of different SDIC tool path patterns may be obtained. In this example, the variation range of the number of the steepest-ascending tool paths is between one and thirty-three. The two extreme cases of the SDIC tool path scheme include:

• One steepest-ascending tool path: In this case the first tool path is the steepest-ascending and thereafter the SDIC tool path scheme becomes an unconstrained isocusped tool path scheme. All but one tool path is generated based upon the iso-cusp principle. These tool paths are shown in Fig. 15, and the tool path length is 5084 mm.

• Thirty-three steepest-ascending tool paths: In this case the number of the steepest-ascending tool path reaches the maximum, because the surface tolerance meets at the base of the half-cylinder and all other areas are over-machined. Under this condition, the SDIC tool path scheme actually becomes the steepest-ascending tool path generation method. Figure 16 illustrates the tool paths, and the tool path length is 5183 mm.

5.4 Machining Results. The hemi-cylinder part is machined using the three SDIC tool path patterns discussed above. A VM-5 Victor 4-axis CNC machining center was used to machine these parts from Ren-Shape corrugated fiberboard. The machined components are shown in Fig. 17. Fig. 17(a) shows the SDIC tool paths with six steepest-ascending tool paths; Fig. 17(b) shows the isocusped tool paths; and Fig. 17(c) shows the steepest-ascending tool paths.

For this example the Iso-Cusped and the Steepest-Ascending tool paths have 14% and 16% longer machining time with respect to the SDIC tool path. The machining time saving of SDIC tool paths will be greater when the surface tolerance is tightened. For a more realistic surface tolerance of 0.01 mm the iso-cusped and steepest-ascending tool paths have 37% and 26% longer machining time with respect to the SDIC tool path. The SDIC tool path and machined component are, for this surface tolerance, shown in Fig. 18.

6 Conclusions

A new tool path planning principle for 3-axis sculptured parts CNC machining, the steepest-ascending tool path that has the

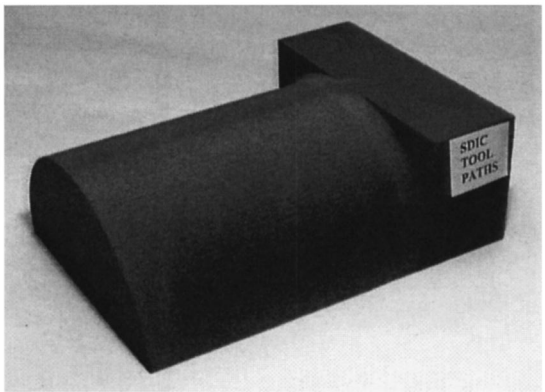

Fig. 18 SDIC tool paths and machined component with surface tolerance 0.01 mm

highest material removal rate in a single tool path, is introduced. The steepest tangent direction of a sculptured surface at a CC point is formulated, and the algorithm for finding the steepest-ascending tool path is provided. If the cutter moves along the steepest tangent direction of the surface in 3-axis CNC milling, the length of the effective cutting edge and the cutting efficiency reach their maximum. The principle serves as a guide in 3-axis CNC tool path planning for complex sculptured surfaces. The steepest-ascending tool paths are integrated into the steepest-directed and iso-cusped (SDIC) tool path generation method to create CNC tool paths for machining sculptured parts with considerably improved global efficiency. Several machining examples using different types of tool paths are used to demonstrate the steepest-ascending and SDIC tool paths, as well as their superior performance in machining efficiency.

Acknowledgment

Financial supports from the Natural Science and Engineering Research Council (NSERC) of Canada are gratefully acknowledged.

References

[1] Choi, B. K., and Jerard, R. B., 1998, *Sculptured Surface Machining: Theory and Application*, Kluwer Academic Publishers.

[2] Broomhead, P., and Edkins, M., 1986, ''Generation NC Data at the Machine Tool for the Manufacture of Free-Form Surfaces,'' Int. J. Prod. Res., **24**(1), pp. 1–14.

[3] Choi, B. K., Lee, C., Huang, J., and Jun, C., 1988, ''Compound Surface Modeling and Machining,'' Comput.-Aided Des., **20**(3), pp. 127–136.

[4] Huang, Y., and Oliver, J. H., 1994, ''Non-Constant Parameter NC Tool Path Generation on Sculptured Surfaces,'' The International Journal of Advanced Manufacturing Technology, **9**, pp. 281–290.

[5] Yang, D. C. H., and Han, Z., 1999, ''Interference Detection and Optimal Tool Selection in 3-Axis NC Machining of Free-Form Surfaces,'' Comput.-Aided Des., **31**, pp. 303–315.

[6] Lin, R., and Koren, Y., 1996, ''Efficient Tool-Path Planning for Machining Free-Form Surfaces,'' ASME J. Ind., **118**, pp. 20–28.

[7] Sarma, R., and Dutta, D., 1997, ''The Geometry and Generation of NC Tool Paths,'' ASME J. Mech. Des., **119**, pp. 253–258.

[8] Suresh, K., and Yang, D. C. H., 1994, ''Constant Scallop Height Machining of Free-Form Surfaces,'' ASME J. Ind., **116**, pp. 253–259.

[9] Maeng, H., Ly, M., and Vickers, G. W., 1996, ''Feature-Based Machining of Curved Surfaces Using the Steepest Directed Tree Approach,'' Journal of Manufacturing Systems, **15**(6), pp. 1–13.

[10] Chen, Z., Dong, Z., and Vickers, G. W., 2003, ''Most Efficient Tool Feed Direction in Three-Axis CNC Machining,'' Journal of Integrated Manufacturing Systems, **14**(7).

[11] Chen, Z., Dong, Z., and Vickers, G. W., 2001, ''Steepest-Directed Tool Path in 3-Axis CNC Machining—The Most Efficient Machining Scheme and its Mathematical Proof,'' *Proceedings of the ASME 2001 Design Engineering Technical Conferences and Computers and Information in Engineering Conference*, *DETC2001/CIE-21301*.

[12] Chen, Z., Vickers, G. W., and Dong, Z., 2003, ''Integrated Steepest-Directed and Iso-Cusped Tool Path Generation for 3-Axis CNC Machining of Sculptured Parts,'' Journal of Manufacturing Systems, **22**(3).

[13] Faux, I. D., and Pratt, M. J., 1979, *Computational Geometry for Design and Manufacture*, Ellis Horwood Limited, West Sussex, England.

[14] Riddle, D. F., 1970, *Calculus and Analytic Geometry*, Wadsworth Publishing Company, Inc., Belmont, California.

[15] Marsden, J., and Weinstein A., 1985, *Calculus III*, Springer-Verlag New York Inc., New York.